

# Generation and confirmation of a $(100 \times 100)$ -dimensional entangled quantum system

Mario Krenn<sup>a,b,1</sup>, Marcus Huber<sup>c,d,e</sup>, Robert Fickler<sup>a,b</sup>, Radek Lapkiewicz<sup>a,b</sup>, Sven Ramelow<sup>a,b,2</sup>, and Anton Zeilinger<sup>a,b,1</sup>

<sup>a</sup>Institute for Quantum Optics and Quantum Information, Austrian Academy of Sciences, A-1090 Vienna, Austria; <sup>b</sup>Vienna Center for Quantum Science and Technology, Faculty of Physics, University of Vienna, A-1090 Vienna, Austria; <sup>c</sup>Department of Mathematics, University of Bristol, Bristol BS8 1TW, United Kingdom; <sup>d</sup>Institut de Ciències Fotoniques, E-08860 Castelldefels (Barcelona), Spain; and <sup>e</sup>Física Teòrica: Informació i Fenòmens Quàntics, Departament de Física, Universitat Autònoma de Barcelona, E-08193 Bellaterra (Barcelona), Spain

Contributed by Anton Zeilinger, February 24, 2014 (sent for review December 15, 2013)

**Entangled quantum systems have properties that have fundamentally overturned the classical worldview. Increasing the complexity of entangled states by expanding their dimensionality allows the implementation of novel fundamental tests of nature, and moreover also enables genuinely new protocols for quantum information processing. Here we present the creation of a  $(100 \times 100)$ -dimensional entangled quantum system, using spatial modes of photons. For its verification we develop a novel nonlinear criterion which infers entanglement dimensionality of a global state by using only information about its subspace correlations. This allows very practical experimental implementation as well as highly efficient extraction of entanglement dimensionality information. Applications in quantum cryptography and other protocols are very promising.**

photonic spatial modes | quantum optics | Schmidt rank | entanglement witness

Quantum entanglement of distant particles leads to correlations that cannot be explained in a local realistic way (1–3). To obtain a deeper understanding of entanglement itself, as well as its application in various quantum information tasks, increasing the complexity of entangled systems is important. Essentially, this can be done in two ways. The first method is to increase the number of particles involved in the entanglement (4). The alternative method is to increase the entanglement dimensionality of a system.

Here we focus on the latter one, namely on the dimension of the entanglement. The text is structured as follows. After a short review of properties and previous experiments, we present a unique method to verify high-dimensional entanglement. Then we show how we experimentally create our high-dimensional two-photon entangled state. We analyze this state with our method and verify a  $100 \times 100$ -dimensional entangled quantum system. We conclude with a short outlook to potential future investigations.

High-dimensional entanglement provides a higher information density than conventional two-dimensional (qubit) entangled states, which has important advantages in quantum communication. First, it can be used to increase the channel capacity via superdense coding (5). Second, high-dimensional entanglement enables the implementation of quantum communication tasks in regimes where mere qubit entanglement does not suffice. This involves situations with a high level of noise from the environment (6, 7), or quantum cryptographic systems where an eavesdropper has manipulated the random number generator involved (8). Moreover, the entangled dimensions of the whole Hilbert space also play a very interesting role in quantum computation: high-dimensional systems can be used to simplify the implementation of quantum logic (9). Furthermore, it has been found recently (10) that any continuous measure of entanglement (such as concurrence, entanglement of formation, or negativity) can be very small, while the quantum system still permits an exponential computation speedup over classical machines. This is not the case for the dimension of entanglement—for every quantum computation, it needs to be high (11, 12), which is another hint at the fundamental relevance of the concept.

So far, high-dimensional entanglement has been implemented only in photonic systems. There, different multilevel degrees of

freedom, such as spatial modes (13), time-energy (14), path (15, 16), as well as continuous variables (17, 18), have been used. Entanglement of spatial modes of photons has especially attracted much attention in recent years (19–28), because it is readily available from optical nonlinear crystals and the number of involved modes of the entanglement can be very high (29).

In a recent experiment the nonseparability of a two-photon state was shown, by observing Einstein–Podolsky–Rosen correlations of photon pairs in down-conversion (30) (for a similar experiment, see ref. 31). The authors were able to observe entanglement of  $\sim 2,500$  spatial states with a camera. In our experiment we go a step further and not only show nonseparability, but we can also extract information about the dimensionality of the entanglement. Precisely, we experimentally verify 100-dimensional entanglement.

One main challenge that remains is the detection and verification of high-dimensional entanglement. For reconstructing the full quantum state via state tomography, the number of required measurements is impractical even for relatively low dimensions because it scales quadratically with the quantum system dimension (24, 27). Even if one had reconstructed the full quantum state, the quantification of the entangled dimensions is a daunting task analytically and even numerically (32). If the full density matrix of the state is not known, it is only possible to give lower bounds of the entangled dimensions. Such methods are usually referred to as a “Schmidt number witness” (33–35).

## Results

In our experiment we are in a regime where it is unfeasible to reconstruct the full density matrix because of the required number

### Significance

Quantum entanglement is one of the key features of quantum mechanics. Quantum systems are the basis of new paradigms in quantum computation, quantum cryptography, or quantum teleportation. By increasing the size of the entangled quantum system, a wider variety of fundamental tests as well as more realistic applications can be performed. The size of the entangled quantum state can increase with the number of particles or, as in the present paper, with the number of involved dimensions. We explore a quantum system that consists of two photons which are 100-dimensionally entangled. The dimensions investigated are the different spatial modes of photons. The result may have potential applications in quantum cryptography and other quantum information tasks.

Author contributions: M.K. and A.Z. designed research; M.K. and R.F. performed research; M.H. contributed new reagents/analytic tools; M.K., M.H., R.F., R.L., S.R., and A.Z. analyzed data; and M.K., M.H., R.F., R.L., S.R., and A.Z. wrote the paper.

The authors declare no conflict of interest.

See Commentary on page 6122.

<sup>1</sup>To whom correspondence may be addressed. E-mail: anton.zeilinger@univie.ac.at or mario.krenn@univie.ac.at.

<sup>2</sup>Present address: School of Applied and Engineering Physics, Cornell University, Ithaca, NY 14853.

This article contains supporting information online at [www.pnas.org/lookup/suppl/doi:10.1073/pnas.1402365111/-DCSupplemental](http://www.pnas.org/lookup/suppl/doi:10.1073/pnas.1402365111/-DCSupplemental).



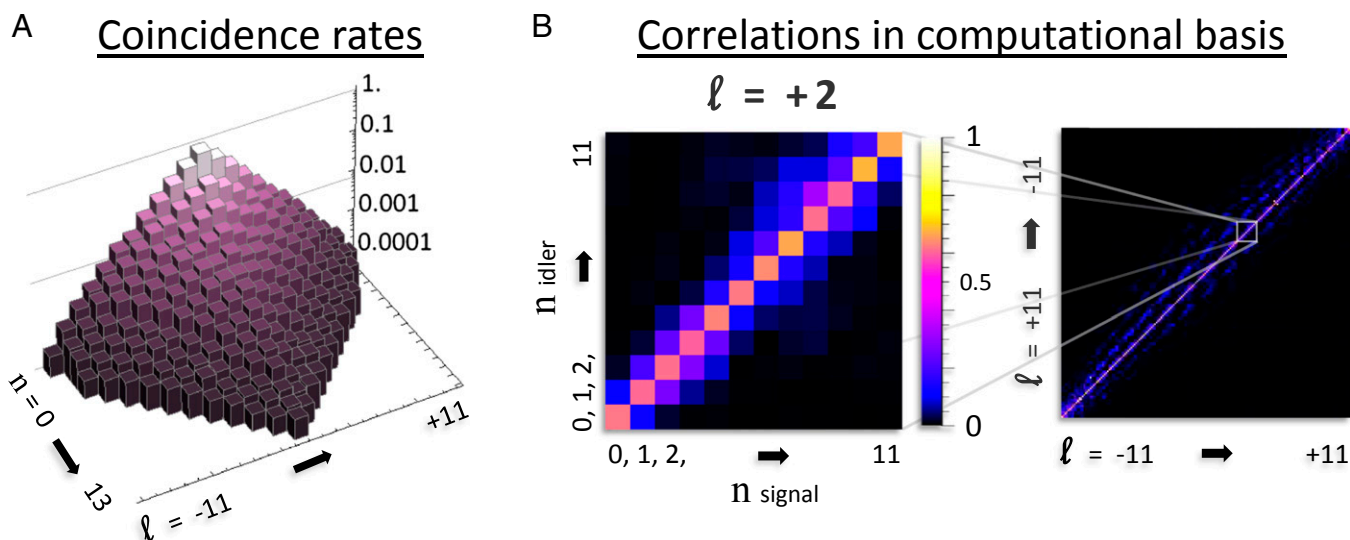


**Fig. 3.** (A) Normalized coincidence rate of different modes (with logarithmic scale), depending on the two mode-numbers (full-field bandwidth). The absolute count rate was 105,500 photon pairs per second for a pump power of 60 mW. To be precise, this is the summed count rate of all 186 modes, not taking into account the inefficiencies of the detectors or imperfect coupling into SMFs. (B) Weighted correlations between different modes in  $z$  basis. Due to different probabilities of different modes, in these pictures we weight every correlation with the probability of the modes involved. That means,  $\langle ij \rangle_{\text{weighted}} = N \langle (ij)_{\text{measured}} / \sqrt{\langle i | i \rangle \langle j | j \rangle} \rangle$ , where  $i$  and  $j$  stand for different two-photon modes, and  $N$  is a normalization constant. (Left) The correlation of modes with  $l = 2$  is shown, and reveals good correlation of modes with the same number of radial nodes. (Right) All correlations in the  $z$  basis are visualized.

MUBs in every two-dimensional subspace. This is represented by the first term on the right side. If the entanglement dimensionality of the state is smaller than that of the observed Hilbert space, the maximally reachable value decreases by  $D$  for each nonentangled dimension ( $D - d$ ), which is expressed by the second term.

The quantity in Eq. 1 is remarkable because the number of required measurements scales only linearly with the dimension of the whole Hilbert space, in contrast to state tomography, which scales quadratically. Furthermore, it only involves measurements in two-dimensional subspaces, which are easier to implement than general high-dimensional measurements. Moreover, the quantity  $W$  in Eq. 1 is nonlinear, which makes it particularly efficient for nonmaximally entangled quantum states (SI Text).

In our experiment, we apply this unique method to a two-photon quantum system. The photon pair is created by pumping a nonlinear crystal with a laser, where spontaneous parametric down-conversion (SPDC) occurs. For the high-dimensional degree

of freedom we use spatial modes of light. Specifically, we use the Laguerre–Gauss (LG) basis to analyze entanglement. LG modes form a basis of solutions of the paraxial wave equation in the cylindrical coordinate system. They are described by two quantum numbers. One quantum number  $l$  corresponds to the orbital angular momentum (OAM, or equivalently, the topological charge) of the photon (38, 39). The second quantum number  $n$  corresponds to the radial nodes in the intensity profile. Only lately this second degree of freedom has been analyzed theoretically in a quantum mechanical framework (40–42).

In the down-conversion process the angular momentum of the photons is conserved, therefore this degree of freedom is anti-correlated. For the radial quantum number  $n$  the situation is more complicated. The full down-conversion process concerning the correlations for the radial quantum number has been analyzed in detail (40) and quasiperfect correlations have been found for specific situations. Recently, these quasiperfect correlations have been demonstrated experimentally (43). The state we expect from

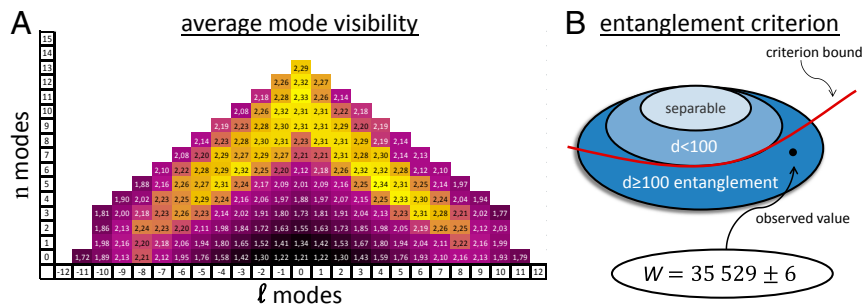


**Fig. 4.** (A) The average sum of visibilities (in  $x$ ,  $y$ , and  $z$  basis) of a specific mode with all other modes is shown. The observable structure originates from nonmaximally entanglement due to different count rates for different modes (Fig. 3A). The bright regions in the center are modes with a similar probability. The central low-order modes (such as the Gauss mode) have the highest probability, therefore the lowest average visibility. Precisely, the Gauss mode has an average sum of visibilities of 1,21 (which mainly results from the visibilities in  $z$  basis). A maximally entangled high-dimensional state would have a summed visibility of 3 for every mode pair. The structure shows that different modes contribute differently to the entanglement criterion. (B) To reveal information about the global, high-dimensional entanglement, we have to calculate the value for the quantity  $W$  in Eq. 1. This is done by summing up all visibilities of all subsets. Here, the concept and result of the entanglement dimensionality criterion is visualized. With our criterion in Eq. 2, quantum states are divided into two parts: those with entanglement dimensionality smaller than 100 and those with a larger one (red line). We have observed a value that lies in the lower part, thus we have verified 100-dimensional entanglement.



down-conversion can then be written as a perfectly (anti)-correlated pure state  $|\psi\rangle = \sum_{n=0}^{\infty} \sum_{l=-\infty}^{\infty} a_{n,l} |LG_{n,l}, LG_{n,-l}\rangle$  with  $l$  and  $n$  dependent coefficients  $a$ . In the derivation of the bounds in Eq. 2 we restricted the states to be perfectly correlated. This means we assume a physical property of our input state, namely perfect (anti)-correlation of the modes. Small deviations from this assumption (which we have observed in the experiment) have been analyzed numerically (*SI Text*), and we found that it only reduces our observed  $W$ , thus justifies the application of the criterion in Eq. 2 in our experiment. The full analytical treatment in the general case is an interesting open problem.

The experimental analysis of the LG modes of the photon pair produced is done by a holographic mode transformation using a spatial light modulator (SLM). With that we can transform any desired mode to a Gauss mode. By using a single-mode fiber (SMF), we filter only for Gauss modes and thereby project the quantum state into the desired mode (39). The setup and exemplary LG modes are shown in Fig. 2.

In our experiment we analyze the correlations of 186 modes of two photons (Fig. 3). The number of modes, 186 in our case, corresponds to  $D$  in Eq. 2. We use LG modes with an angular quantum number up to  $l = 11$ , and a radial quantum number up to  $n = 13$ . To calculate the quantity in Eq. 1, we need to measure in every two-dimensional subspace [there are  $(186 \times 185)/2 = 17,205$  two-dimensional subspaces] the visibility in  $x$ ,  $y$ , and  $z$  basis, which corresponds to  $3 \times 4$  measurement per subspace. Altogether this results in  $\sim 200,000$  measurements (with  $\sim 750$  million detected photon pairs). For comparison, if we had performed a full state tomography, we would have needed to perform more than 1 billion measurements. When we sum up all of our measured visibilities according to Eq. 1, we find

$$W_{D=186} = 35,529 \pm 6, \quad [3]$$

which corresponds to at least 100-dimensional entanglement according to inequality 2 (101-dimensional:  $W > 35,619$ ; 100-dimensional:  $W > 35,433$ ; 99-dimensional:  $W > 35,247$ ). The confidence interval corresponds to one SD due to the statistical uncertainty. It has been calculated using Monte Carlo simulation assuming Poisson distribution of the count rates. The detailed measurement results and the calculation of [3] can be seen in Fig. 4 and in *SI Text*. The quantity  $W$  in [1] corresponds to measurements of all two-dimensional subspaces in a  $D \times D$ -dimensional quantum state. It can be seen in Fig. 44 that some modes contribute more to the quantity than others, thus we can try to find a smaller optimal set of modes that shows the higher-dimensional entanglement. We find that by removing 19 modes (that means, not taking into account all two-dimensional subspace measurements with them), we can find at least 103-dimensional entanglement.

One way to bring this in relation with other photonic and multipartite entanglement experiments is the following. The

dimension of the entangled Hilbert-space scales with  $\dim = d^N$ , where  $d$  stands for the entangled dimensions and  $N$  is the number of involved parties. Our experiment shows an entangled Hilbert-space dimension of  $\dim = (103 \times 103) \approx 2^{13.4}$  that is larger than the largest entangled photonic Hilbert space reported so far (with  $\dim = 2^{10}$ ) (44). Interestingly, it is of similar magnitude as that of the largest quantum systems with multipartite entanglement measured so far, such as 14-qubit ion entanglement with  $\dim = 2^{14}$  (45).

## Discussion

Our results show that we can experimentally access a quantum state of two photons which is at least  $(100 \times 100)$ -dimensionally entangled. This was possible by developing a unique method to analyze efficiently and in an experimentally practical way quantum states with very high dimensions. Furthermore, we exploited the full potential of transverse spatial modes, namely both radial and angular quantum numbers.

Such high-dimensional entanglement offers a great potential for quantum information applications. There are situations where two-dimensional entanglement is no longer sufficient but high-dimensional entangled systems are able to perform the task. In realistic quantum cryptography schemes, for example where noisy environment or manipulated random number generators lead to a breakdown of the system for low-dimensional entangled states, high-dimensionality of the entanglement sustains the security (6–8). The experimental setups as presented here are suitable for such tasks. Additionally, for quantum computation it is necessary to use a large entangled Hilbert space for any quantum speedup. As our result shows that very high-dimensional entangled Hilbert spaces are experimentally accessible, we envision that it will trigger future experiments to solve the next important open question: How to implement experimentally arbitrary controlled transformations between spatial modes to realize quantum computational or similar tasks.

**ACKNOWLEDGMENTS.** We thank Christoph Schäff, Mehul Malik, and William Plick for helpful discussions. M.K. thanks the quantum information theory groups at Institut de Ciències Fotòniques (ICFO) and Universitat Autònoma de Barcelona (UAB) and M.H. for hospitality. M.H. acknowledges productive discussions of the entanglement detection criterion with Ariel Bendersky, Stephen Brierley, Jonathan Bohr-Brask, Daniel Cavalcanti, Otfried Gühne, Karen Hovhannisyán, Claude Klöckl, Milan Mosonyi, Marcin Pawłowski, Martin Plesch, Paul Skrzypczyk, and Andreas Winter. This work was supported by the European Research Council [(ERC) Advanced Grant 227844 QIT4QAD (photonic quantum information technology and the foundations of quantum physics in higher dimensions); Simulators and Interfaces with Quantum Systems, 600645 European Union (EU) Seventh Framework Programme Information and Communication Technologies] and the Austrian Science Fund FWF with the Spezialforschungsbereich (SFB) F40 [Foundations and Applications of Quantum Science (FoQus)] and W1210-2 [Complex Quantum Systems (CoQus)]. M.H. also acknowledges Marie Curie Intra-European Fellowships for Career Development Grant QuaCoCoS-302021 and S.R. acknowledges EU Marie Curie Fellowship PIOF-GA-2012-329851.

- Einstein A, Podolsky B, Rosen N (1935) Can quantum-mechanical description of physical reality be considered complete? *Phys Rev* 47(10):777.
- Schrödinger E (1935) Probability relations between separated systems. *Proc Camb Philos Soc* 31:555–563.
- Bell JS (1964) On the Einstein-Podolsky-Rosen paradox. *Physics* 1:195–200.
- Greenberger DM, Horne MA, Shimony A, Zeilinger A (1990) Bell's theorem without inequalities. *Am J Phys* 58(12):1131–1143.
- Wang C, Deng F-G, Li Y-S, Liu X-S, Long GL (2005) Quantum secure direct communication with high-dimension quantum superdense coding. *Phys Rev A* 71(4):044305.
- Lloyd S (2008) Enhanced sensitivity of photodetection via quantum illumination. *Science* 321(5895):1463–1465.
- Zhang Z, Tengner M, Zhong T, Wong FNC, Shapiro JH (2013) Entanglement's benefit survives an entanglement-breaking channel. *Phys Rev Lett* 111(1):010501.
- Huber M, Pawłowski M (2013) Weak randomness in device independent quantum key distribution and the advantage of using high dimensional entanglement. *Phys Rev A* 88(3):032309.
- Lanyon BP, et al. (2009) Simplifying quantum logic using higher-dimensional Hilbert spaces. *Nat Phys* 5(2):134–140.
- Van den Nest M (2013) Universal quantum computation with little entanglement. *Phys Rev Lett* 110(6):060504.
- Vidal G (2003) Efficient classical simulation of slightly entangled quantum computations. *Phys Rev Lett* 91(14):147902.
- Jozsa R, Linden N (2003) On the role of entanglement in quantum-computational speed-up. *Proc R Soc A* 459(2036):2011–2032.
- Vaziri A, Weihs G, Zeilinger A (2002) Experimental two-photon, three-dimensional entanglement for quantum communication. *Phys Rev Lett* 89(24):240401.
- Richard D, Fischer Y, Weinfurter H (2012) Experimental implementation of higher dimensional time-energy entanglement. *Appl Phys B* 106(3):543.
- Rossi A, Vallone G, Chiuri A, De Martini F, Mataloni P (2009) Multipath entanglement of two photons. *Phys Rev Lett* 102(15):153902.
- Schaeff C, et al. (2012) Scalable fiber integrated source for higher-dimensional path-entangled photonic qNits. *Opt Express* 20(15):16145.
- Yokoyama S, et al. (2013) Ultra-large-scale continuous-variable cluster states multiplexed in the time domain. *Nat Photonics* 7(12):982–986.
- Fabre C, Treps N, Roslund J, Medeiros de Araujo R, Jiang S (2013) Parametrically generated ultrafast frequency combs: A promising tool for wavelength multiplexed quantum information processing. *The Rochester Conferences on Coherence and Quantum Optics* (Optical Society of America, Washington). Available at [www.opticsinfobase.org/abstract.cfm?uri=CQO-2013-W2A.1](http://www.opticsinfobase.org/abstract.cfm?uri=CQO-2013-W2A.1). Accessed March 2014.

19. Molina-Terriza G, Vaziri A, Reháček J, Hradil Z, Zeilinger A (2004) Triggered qutrits for quantum communication protocols. *Phys Rev Lett* 92(16):167903.
20. Langford NK, et al. (2004) Measuring entangled qutrits and their use for quantum bit commitment. *Phys Rev Lett* 93(5):053601.
21. Molina-Terriza G, Vaziri A, Ursin R, Zeilinger A (2005) Experimental quantum coin tossing. *Phys Rev Lett* 94(4):040501.
22. Pors JB, et al. (2008) Shannon dimensionality of quantum channels and its application to photon entanglement. *Phys Rev Lett* 101(12):120502.
23. Dada AC, Leach J, Buller GS, Padgett MJ, Andersson E (2011) Experimental high-dimensional two-photon entanglement and violations of generalized Bell inequalities. *Nat Phys* 7(9):677–680.
24. Agnew M, Leach J, McLaren M, Roux FS, Boyd RW (2011) Tomography of the quantum state of photons entangled in high dimensions. *Phys Rev A* 84(6):062101.
25. Romero J, Giovannini D, Franke-Arnold S, Barnett SM, Padgett MJ (2012) Increasing the dimension in high-dimensional two-photon orbital angular momentum entanglement. *Phys Rev A* 86(1):012334.
26. McLaren M, et al. (2012) Entangled Bessel-Gaussian beams. *Opt Express* 20(21):23589–23597.
27. Giovannini D, et al. (2013) Characterization of high-dimensional entangled systems via mutually unbiased measurements. *Phys Rev Lett* 110(14):143601.
28. Pimenta WM, et al. (2013) Minimum tomography of two entangled qutrits using local measurements of one-qutrit symmetric informationally complete positive operator-valued measure. *Phys Rev A* 88(1):012112.
29. Svozilik J, Peřina J, Torres JP (2012) High spatial entanglement via chirped quasi-phase-matched optical parametric down-conversion. *Phys Rev A* 86(5):052318.
30. Edgar MP, et al. (2012) Imaging high-dimensional spatial entanglement with a camera. *Nat Commun* 3:984.
31. Moreau PA, Mougin-Sisini J, Devaux F, Lantz E (2012) Realization of the purely spatial Einstein-Podolsky-Rosen paradox in full-field images of spontaneous parametric down-conversion. *Phys Rev A* 86(1):010101.
32. Gurvits L (2003) Classical deterministic complexity of Edmonds' problem and quantum entanglement. *Proceedings of the 35th Annual ACM Symposium on Theory of Computing* (ACM, San Diego), pp 10–19.
33. Terha BM, Horodecki P (2000) Schmidt number for density matrices. *Phys Rev A* 61(4):040301.
34. Sanpera A, Bruß D, Lewenstein M (2001) Schmidt-number witnesses and bound entanglement. *Phys Rev A* 63(5):050301.
35. Gühne O, Toth G (2009) Entanglement detection. *Phys Rep* 474(1):1–75.
36. Krenn M, et al. (2013) Entangled singularity patterns of photons in Ince-Gauss modes. *Phys Rev A* 87(1):012326.
37. Agnew M, Salvail JZ, Leach J, Boyd RW (2013) Generation of orbital angular momentum Bell states and their verification via accessible nonlinear witnesses. *Phys Rev Lett* 111(3):030402.
38. Allen L, Beijersbergen MW, Spreeuw RJC, Woerdman JP (1992) Orbital angular momentum of light and the transformation of Laguerre-Gaussian laser modes. *Phys Rev A* 45(11):8185–8189.
39. Mair A, Vaziri A, Weihs G, Zeilinger A (2001) Entanglement of the orbital angular momentum states of photons. *Nature* 412(6844):313–316.
40. Miatto FM, Yao AM, Barnett SM (2011) Full characterization of the quantum spiral bandwidth of entangled biphotons. *Phys Rev A* 83(3):033816.
41. Karimi E, Santamato E (2012) Radial coherent and intelligent states of paraxial wave equation. *Opt Lett* 37(13):2484–2486.
42. Plick WN, Lapkiewicz R, Ramelow S, Zeilinger A (2013) . The Forgotten Quantum Number: A short note on the radial modes of Laguerre-Gauss beam. arXiv:1306.6517.
43. Salakhutdinov VD, Eliel ER, Löffler WL (2012) Full-field quantum correlations of spatially entangled photons. *Phys Rev Lett* 108(17):173604.
44. Gao W-B, et al. (2010) Experimental demonstration of a hyper-entangled ten-qubit Schrödinger cat state. *Nat Phys* 6(5):331–335.
45. Monz T, et al. (2011) 14-Qubit entanglement: Creation and coherence. *Phys Rev Lett* 106(13):130506.